Radio Propagation Environment Prediction Method for UAV-assisted Cellular Networks with Millimeter-wave Beamforming

Shunsuke Fujio and Kazuyuki Ozaki
Fujitsu Limited
4-1-1 Kamikodanaka, Nakahara-ku, Kawasaki-shi, Kanagawa 211-8588, Japan

***Abstract*—This paper considers an unmanned aerial vehicle (UAV)-assisted millimeter-wave cellular network system. This system can provide a high frequency communication area around a user equipment (UE) by moving a relay station (RS) mounted on the UAV to an appropriate position and relaying signals. The RS communicates with the UE and a base station using narrow beams to compensate for large propagation loss in high frequency bands. Accurate prediction of the propagation environment is important for determining where to move the UAV-RS in this system. Therefore, we propose a radio propagation prediction method that utilizes received power information for multiple beams. The proposed method estimates the propagation conditions and parameters for measurement data by considering not only the relationship between distance and received power but also the power ratio between the beams. Subsequently, a blockage map indicating where a signal is blocked is constructed based on the estimated results. The propagation condition and the channel gain at a given position pair can be predicted using the estimated parameters and the constructed blockage map. Computer simulation results, assuming an urban environment, demonstrate that the proposed method can accurately predict the propagation environment even when there is a large variation in the received power.**

Keywords—UAV, relay communication, radio propagation environment prediction, millimeter-wave, beamforming

I. INTRODUCTION

Wireless communication on high frequency bands such as millimeter-wave bands has been specified for the fifth-generation (5G) New Radio and large capacity cellular systems utilizing large bandwidth in the high frequency bands have been realized [1]. In the sixth-generation (6G) era, many use cases that require much larger system capacity such as a holographic communication, a digital twin and an extended reality are expected to be enabled [2]. Therefore, the use of the high frequency bands is still an essential component to accommodate the huge traffic required in the 6G era [1] [2].

However, coverage enhancement is challenging in the high frequency band communication due to large propagation loss and a blockage effect by obstacles such as buildings. In particular, since it is hard for a user equipment (UE) to increase transmission power considering its portability, unlike a base station (BS), an area where high data rate can be achieved at uplink is limited [3]. Although the received signal power can be improved by densely BS deployment, it is not desirable to deploy a large number of BSs from the viewpoint of installation cost and power consumption.

Therefore, we have been studying a unmanned aerial vehicle (UAV)-assisted cellular network system to improve uplink communication performance in the high frequency bands [4]. This system can provide a high frequency communication area around the user by moving a relay station (RS) mounted on the UAV to an appropriate position based on the UE position information and relaying signals between the BS and UE. The RS has a beamforming architecture and communicates with the UE and BS using narrow beams to compensate for large propagation loss. In this system, a radio propagation environment prediction is key factor to determine the destination of UAV-RS. Depending on a position pair of the UE and UAV-RS, signal quality may deteriorate due to, for example, a blockage of a line-of-sight (LOS) path. Therefore, it is important to know the radio propagation environment of the destination before moving.

Radio propagation environment prediction methods have been studied in [5]-[10]. In [5], a Gaussian process based prediction method was proposed. In [6], a deep learning approach was studied to predict the propagation conditions, such as LOS and non-LOS (NLOS), and the channel gain. In [7]-[10], methods to estimate propagation parameters, such as path-loss exponent, for each propagation condition and then predict the channel gain based on the estimation results were proposed. Authors in [7] proposed a method to estimate the propagation condition for each measurement result and the propagation parameters by using the expectation-maximization (EM) algorithm. In [8], a method to construct a blockage map indicating where a signal is blocked based on the propagation condition estimation results was proposed to predict the propagation condition at a given position pair. In [9], a method to alternatively optimize the propagation parameters and the blockage map was proposed. In [10], authors utilized not only radio-related information but also depth image information to construct the blockage map.

However, beamforming has not been considered in any of the above papers. In our system where the beamforming technology is applied to the UAV-RS, different received power information can be obtained for each beam even if the position pair of the UE and UAV-RS is the same. Therefore, we propose a radio propagation prediction method that utilizes received power information for multiple beams. The proposed method estimates the propagation conditions and parameters for the measurement data by considering not only the relationship between distance and received power but also the power ratio between the beams. The estimation accuracy can be expected to improve by utilizing the relationship between the power ratio and the propagation condition, for example, the power is concentrated in the beam pointing in the direct wave direction in the LOS case. Subsequently, the blockage map is constructed based on the estimation results, similar to [10]. The propagation condition and the channel gain at a given position pair can be predicted using the estimated parameters and the blockage map. Computer simulation results, assuming an urban environment, demonstrate that the proposed method can accurately predict the propagation environment even when there is a large variation in the received power.

979-8-3503-7099-7/24/$31.00 ©2024 IEEE

The rest of this paper is organized as follows: Our assumed system model is described in Section II. The proposed method is introduced in Section III. The evaluation results are shown in Section IV and conclusions are presented in Section V.

Notation: **a** is a vector, **A** is a matrix, $\mathbf{A}^H$ is the conjugate transpose of matrix **A**.

II. System Model

This paper considers the communication between a UAV-RS and N_{UE} outdoor UEs in an urban environment where users are surrounded by square-shaped buildings as shown in Fig. 1. The RS has a uniform rectangular array (URA) for beamforming, and the UE has an omni-directional antenna.

The RS collects reference signal received power (RSRP) information from all UEs at each of the N_{RS} measurement positions. At each measurement position, the RS transmits a reference signal using each of the B beams, and the UE reports the RSRP information measured for each beam to the RS. The RS stores a set of the RSRP information for all beams and the position information of the UE and RS, for each RS-UE position pair. The number of measurement position pairs is denoted by N and $N = N_{RS}N_{UE}$.

A received signal for the b-th beam at the n-th position pair is given by

$$r_{n,b}(t) = 10^{\frac{P_{TX}+\gamma}{20}}\mathbf{h}_n^H\mathbf{w}_b s(t) + \xi(t), \quad (1)$$

where $P_{TX}, \gamma, \mathbf{h}_n, \mathbf{w}_b, s$, and ξ denote the transmission power in dB, the channel gain in dB including path-loss and shadowing effect, the channel vector, the beam weight vector, the reference signal which satisfies $E[|s(t)|^2] = 1$, and the zero-mean additive white Gaussian noise, respectively. The channel vector can be modeled as

$$\mathbf{h}_n = \sum_{l=1}^{N_{path}} c_{n,l}\mathbf{a}(\boldsymbol{\phi}_{n,l}), \quad (2)$$

where N_{path} and $\mathbf{a}(\boldsymbol{\phi})$ denote the number of path components and the array response vector, respectively. $c_{n,l}$ and $\boldsymbol{\phi}_{n,l}$ denote the complex path gain and the departure angle vector, which consists of the azimuth angle of departure (AoD) and the zenith angle of departure (ZoD), of the l-th path at the n-th position pairs, respectively. The AoD and ZoD of the direct wave path is given based on the direction to the UE from the RS, and those of the other paths are given by the wrapped-Gaussian distribution and Laplacian distribution based on the channel model in [11], respectively. The path gain is given by a zero-mean complex Gaussian distribution and the mean power of each path is normalized that the sum of the power is equal to one.

The RSRP for the b-th beam at the n-th position pair is given by the following equation, according to [12].

$$RSRP_{n,b} = 10^{\frac{P_{TX}+\gamma}{10}}\sum_{l=1}^{N_{path}}|c_{n,l}|^2 G_b(\boldsymbol{\phi}_{n,l}), \quad (3)$$

where $G_b(\boldsymbol{\phi})$ denotes the beamforming gain of the b-th beam and is written by

$$G_b(\boldsymbol{\phi}_{n,l}) = |\mathbf{a}^H(\boldsymbol{\phi}_{n,l})\mathbf{w}_b|^2, \quad (4)$$

Note that we assume that the noise is eliminated owing to long-term measurement. Let $\boldsymbol{\rho}$ be the 6-dimension vector which indicates the pair of the RS and UE positions. Generally, as described in [7], the channel gain is modelled as

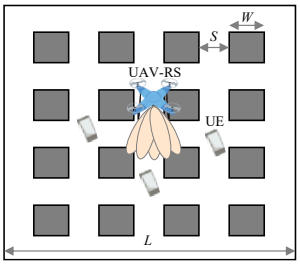

Fig. 1. Illustration of the system model in the urban environment.

$$\gamma = -\alpha \cdot 10\log_{10} d(\boldsymbol{\rho}) + \beta + \zeta, \quad (5)$$

where α, β, ζ, and $d(\boldsymbol{\rho})$ denote the path-loss exponent, the mean channel gain at a reference point, the shadowing component, and the RS-UE distance, respectively. The shadowing effect is modeled as the Gaussian distribution with zero-mean and variance σ^2. Here, the propagation parameters (α, β, σ) are different for each propagation condition.

In this study, we assumed an environment where a LOS path was blocked only by buildings and a propagation condition was uniquely given according to an RS-UE position pair, similar to [7]. Under this assumption, the probability density function of the channel gain is given by

$$p(\gamma) = \mathcal{N}\big(\gamma|\alpha_{k(\boldsymbol{\rho})}, \beta_{k(\boldsymbol{\rho})}, \sigma_{k(\boldsymbol{\rho})}, 10\,log_{10}\,d(\boldsymbol{\rho})\big), \quad (6)$$

where $k(\boldsymbol{\rho})$ and $\mathcal{N}(\gamma|\alpha, \beta, \sigma, D)$ denote the propagation condition for $\boldsymbol{\rho}$ and the probability density function of the Gaussian distribution with mean $\bar{\gamma} = -\alpha D + \beta$ and variance σ^2. The number of propagation conditions is denoted by K, and $K = 2$ in this study (i.e., LOS/NLOS).

The problem in this paper is to predict the channel gain for a given position pair based on the measurement data. Note that we assumed the position information can be obtained with high accuracy by the global navigation satellite system and treated it as known value.

III. Proposed Method

This section describes the details of the proposed propagation environment prediction method. The proposed method learns the propagation environment based on the measurement data and then predicts. First, the propagation condition for each position pair and the propagation parameters for each condition are estimated. Next, the blockage map is constructed based on the estimated results. After that, the propagation condition and the channel gain at a given position pair can be predicted by using the estimated propagation parameters and the constructed blockage map. The overview of the proposed method is shown in Fig. 2.

A. Estimation of the propagaton conditions and parameters

Let y_n and $\mathbf{z}_n$ be the measured channel gain and the one-hot label vector for the propagation condition at the n-th position pair, respectively. The k-th element of $\mathbf{z}_n$, which is $z_{n,k}$, is one if and only if the propagation condition is k at the n-th position pair, otherwise, $z_{n,k} = 0$. The conditional probability density function of y_n given $\mathbf{z}_n$ is given as

$$p(y_n|\mathbf{z}_n) = \prod_{k=1}^{K}\big(\mathcal{N}_{n,k}\big)^{z_{n,k}}, \quad (7)$$

where

$$\mathcal{N}_{n,k} = \mathcal{N}(y_n|\alpha_k, \beta_k, \sigma_k, D_n), \quad (8)$$

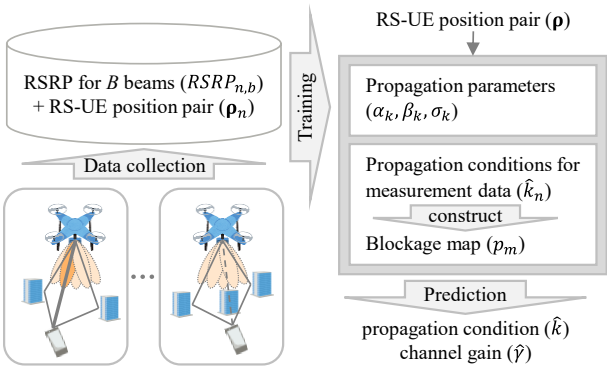

Fig. 2. Overview of the proposed method.

$$D_n = 10\log_{10} d(\boldsymbol{\rho}_n). \tag{9}$$

$\boldsymbol{\rho}_n$ denotes the n-th position pair. In the estimation process, since $\mathbf{z}_n$ is unknown, we treat $\mathbf{z}_n$ as a random variable vector according to the following probability density function, in which the probability that $z_{n,k} = 1$ is denoted as $\pi_{n,k}$.

$$p(\mathbf{z}_n) = \prod_{k=1}^{K} (\pi_{n,k})^{z_{n,k}}, \tag{10}$$

where $\sum_{k=1}^{K} \pi_{n,k} = 1$. Here, the proposed method determines $\pi_{n,k}$ by exploiting the relationship between the power ratio between the beams and the propagation condition. For example, in the LOS case, since a strong direct wave path can be received, the measured RSRP for the beam pointing in the direct wave direction is expected to be much higher than others. On the other hand, in the NLOS case where the direct wave path is blocked, the measured RSRP is distributed across various beams. Therefore, we define the beam power ratio as the ratio of the RSRP of the beam pointing to the direct wave direction to the total RSRP of all beams, and give $\pi_{n,k}$ as a function of the beam power ratio as follows.

$$\pi_{n,1} = \frac{1}{1+\exp(\psi_2\omega_n+\psi_1)} \stackrel{\text{def}}{=} \pi(\omega_n, \boldsymbol{\psi}), \tag{11}$$

$$\pi_{n,2} = 1 - \pi(\omega_n, \boldsymbol{\psi}), \tag{12}$$

where $\boldsymbol{\psi} = [\psi_1, \psi_2]^T$ denotes the weight parameter vector and ω_n denotes the beam power ratio at the n-th position pair. ω_n is calculated as

$$\omega_n = 10\log_{10} \frac{RSRP_{n,b_n}}{\sum_{b=1}^{B} RSRP_{n,b}}, \tag{13}$$

where b_n denotes the index of the beam pointing to the direct wave path. b_n is given as

$$b_n = \underset{b}{\operatorname{argmax}}\, G_b(\hat{\boldsymbol{\Phi}}_n), \tag{14}$$

where $\hat{\boldsymbol{\Phi}}_n$ denote the vector of the direct wave path directions in the azimuth and zenith domains. These directions can be calculated from the position pair information.

The proposed method estimates the parameter set $\theta = \{\alpha_k, \beta_k, \sigma_k, \psi_1, \psi_2\}$ to maximize the log-likelihood function. The likelihood function is given by

$$p(Y|\theta) = \prod_{n=1}^{N} \sum_{k=1}^{K} \pi_{n,k}\mathcal{N}_{n,k}, \tag{15}$$

where Y denotes the set of the channel gain. The problem to be solved is written by

$$\hat{\theta} = \underset{\theta}{\operatorname{argmax}} \ln p(Y|\theta). \tag{16}$$

Note that $\pi_{n,k}$ in (11) and (12) is always satisfy the constraint that $\sum_{k=1}^{K} \pi_{n,k} = 1$, thus the constraint is removed in the problem. Here, since the channel gain cannot be measured directly, we calculate the channel gain from the measured RSRP as

$$y_n = 10\log_{10} \frac{\sum_{b=1}^{B} RSRP_{n,b}}{\sum_{b=1}^{B} G_b(\hat{\boldsymbol{\Phi}}_n)} - P_{TX}. \tag{17}$$

To solve the problem, we introduce $q(Z)$ as the distribution function of Z which is the set of $\mathbf{z}_n$ and define the function $\mathcal{L}(q, \theta)$ as follow.

$$\mathcal{L}(q, \theta) = \sum_Z q(Z) \cdot \ln \frac{p(Y, Z|\theta)}{q(Z)} \tag{18}$$

Here, according to [13], the following equation is satisfied.

$$\ln p(Y|\theta) = \mathcal{L}(q, \theta) - \sum_Z q(Z) \cdot \ln \frac{p(Z|Y, \theta)}{q(Z)} \tag{19}$$

In (19), since the second term of the right side is always zero or less, $\mathcal{L}(q, \theta)$ gives the lower bound of the log-likelihood. Therefore, the problem (16) can be solved by iterating the expectation step (E-step) and the maximization step (M-step) in the well-known EM algorithm [13] as follows.

Suppose that the current parameter set is $\theta^{(t)}$ in the t-th iteration. In the E-step, $\mathcal{L}(q, \theta^{(t)})$ is miximized with respect to $q(Z)$ while fixing $\theta = \theta^{(t)}$. When $q(Z)$ is equal to the following posterior distribution, the second term in (19) is to be zero, then the maximum $\mathcal{L}(q, \theta^{(t)})$ can be achieved.

$$p(Z|Y, \theta^{(t)}) = \frac{p(Y, Z|\theta^{(t)})}{p(Y|\theta^{(t)})} = \prod_{n=1}^{N} \frac{\prod_{k=1}^{K} (\pi_{n,k}\mathcal{N}_{n,k})^{z_{n,k}}}{\sum_{k=1}^{K} \pi_{n,k}\mathcal{N}_{n,k}}. \tag{20}$$

In the M-step, $\mathcal{L}(q^{(t)}, \theta)$ is maximized with respect to θ while fixing $q^{(t)} = p(Z|Y, \theta^{(t)})$. By substituting $q^{(t)}$ to (18), the following equation is obtained.

$$\begin{aligned}\mathcal{L}(q^{(t)}, \theta) = Q(\theta, \theta^{(t)}) \\ - \sum_Z p(Z|Y, \theta^{(t)}) \cdot \ln p(Z|Y, \theta^{(t)}),\end{aligned} \tag{21}$$

where

$$\begin{aligned}Q(\theta, \theta^{(t)}) &\stackrel{\text{def}}{=} \sum_Z p(Z|Y, \theta^{(t)}) \cdot \ln p(X, Z|\theta) \\ &= \sum_{n=1}^{N} \sum_{k=1}^{K} \bar{z}_{n,k}^{(t+1)} (\ln \pi_{n,k} + \ln \mathcal{N}_{n,k}).\end{aligned} \tag{22}$$

Here, $\bar{z}_{n,k}^{(t+1)}$ denotes the responsibility of the Gaussian mixture model. Since the posterior distribution is independent for each data in (20), $\bar{z}_{n,k}^{(t+1)}$ is given by

$$\begin{aligned}\bar{z}_{n,k}^{(t+1)} &\stackrel{\text{def}}{=} \sum_Z z_{n,k} p(Z|Y, \theta^{(t)}) = \\ \sum_{z_n} z_{n,k} p(z_n|y_n, \theta^{(t)}) &= \frac{\pi_{n,k}\mathcal{N}_{n,k}}{\sum_{j=1}^{K} \pi_{n,j}\mathcal{N}_{n,j}}.\end{aligned} \tag{23}$$

Since the second term of the right side in (21) does not depend on θ, the problem in the M-step can be written by

$$\theta^{(t+1)} = \underset{\theta}{\operatorname{argmax}}\, Q(\theta, \theta^{(t)}). \tag{24}$$

The optimum values of α_k, β_k, and σ_k can be obtained by the following equations, similar to [7].

$$\begin{bmatrix} \alpha_k^{(t+1)} \\ \beta_k^{(t+1)} \end{bmatrix} = \mathbf{A}^{-1}\mathbf{b}, \tag{25}$$

$$\sigma_k^{(t+1)} = \sqrt{\frac{\sum_{n=1}^{N} \bar{z}_{n,k}^{(t+1)} \left\{ y_n + \alpha_k^{(t+1)} D_n - \beta_k^{(t+1)} \right\}^2}{\sum_{n=1}^{N} \bar{z}_{n,k}^{(t+1)}}}, \quad (26)$$

where

$$\mathbf{A} = \begin{bmatrix} \sum_{n=1}^{N} \bar{z}_{n,k}^{(t+1)} D_n^2 & -\sum_{n=1}^{N} \bar{z}_{n,k}^{(t+1)} D_n \\ -\sum_{n=1}^{N} \bar{z}_{n,k}^{(t+1)} D_n & \sum_{n=1}^{N} \bar{z}_{n,k}^{(t+1)} \end{bmatrix}, \quad (27)$$

$$\mathbf{b} = \begin{bmatrix} -\sum_{n=1}^{N} \bar{z}_{n,k}^{(t+1)} D_n y_n \\ \sum_{n=1}^{N} \bar{z}_{n,k}^{(t+1)} y_n \end{bmatrix}. \quad (28)$$

For $\boldsymbol{\psi}$, the local optimum value can be achieved by using the gradient descent method to the problem that $\min_{\boldsymbol{\psi}}(-Q)$. The update process is written by $\boldsymbol{\psi} \leftarrow \boldsymbol{\psi} - \eta \boldsymbol{\psi}'$, where η is the learning rate and

$$\boldsymbol{\psi}' = \frac{\partial(-Q)}{\partial \boldsymbol{\psi}} = \begin{bmatrix} \sum_{n=1}^{N} \bar{\psi}_n^{(t+1)} \\ \sum_{n=1}^{N} \omega_n \bar{\psi}_n^{(t+1)} \end{bmatrix}, \quad (29)$$

$$\bar{\psi}_n^{(t+1)} = \bar{z}_{n,1}^{(t+1)} \left(1 - \pi(\omega_n, \boldsymbol{\psi})\right) - \bar{z}_{n,2}^{(t+1)} \pi(\omega_n, \boldsymbol{\psi}), \quad (30)$$

The initial value is given by

$$\boldsymbol{\psi}_0 = \left[\ln \frac{\sum_{n=1}^{N} \bar{z}_{n,2}^{(t+1)}}{\sum_{n=1}^{N} \bar{z}_{n,1}^{(t+1)}}, 0 \right]^T. \quad (31)$$

Note that when using $\boldsymbol{\psi} = \boldsymbol{\psi}_0$, $\pi_{n,k}$ is independent for ω_n and is written by substituting (31) to (11) and (12) as the following equation, which is the same definition used in [7].

$$\pi_{n,k}^{(t+1)} = \frac{1}{N} \sum_{n=1}^{N} \bar{z}_{n,k}^{(t+1)} \; \forall n. \quad (32)$$

After convergence, the propagation condition k_n for each position pair is estimated by

$$k_n = \underset{k}{\operatorname{argmax}} \, \bar{z}_{n,k}. \quad (33)$$

Here, which value of k corresponds to LOS is uncertain in this process, thus, in the proposed method, the value of k for which the path-loss exponent α_k is the nearest to the free space path-loss exponent which is two is regarded as LOS and denoted by $k^{(LOS)}$. The value of k corresponding to NLOS is denoted by $k^{(NLOS)}$.

B. Constructon of the blockage map

Based on the estimated propagation conditions, the proposed method constructs the blockage map. To construct it, the evaluation space is partitioned into individual grids of equal volume where each grid is identified by the index m. p_m denotes the blockage probability at the m-th grid.

The basic concept of the map construction is to assign a low probability to grids on a straight path between the UE and RS where the propagation condition is LOS, assuming that there are no obstacles on the path, similar to [10]. However, if some of the estimated propagation conditions are incorrect, a low blockage probability may be assigned to a grid where there is an obstacle and a signal is actually blocked. Therefore, the proposed method also considers NLOS data and increases the blockage probability at grids on an NLOS path to compensate for the negative effect of the misestimation from NLOS to LOS. Additionally, the use of incorrect data is suppressed by selecting data for the map construction according to their responsibility $\bar{z}_{n,k}$.

The map is constructed as follows. First, the data of which responsibility corresponding to the estimated condition is equal to or greater than a threshold λ is selected for the map construction. Next, the map is initialized by assigning an initial value above 0.5 to all grids. Finally, the map is updated according to the propagation condition and the RS-UE path of each of the selected data. Similar to [10], for LOS path data, all grids above or on the path are updated under the assumption that there are no obstacles above the LOS path. For NLOS, all grids below or on the path are updated. The map updated by the n-th data is given as

$$p_m \leftarrow \begin{cases} \left(1 + \frac{1-p_m}{p_m} \cdot \frac{1-\mu_n}{\mu_n}\right)^{-1}, & \left(if \; m \in \bar{\mathcal{M}}(\boldsymbol{\rho}_n)\right) \\ p_m, & (otherwise) \end{cases}, \quad (34)$$

where $\bar{\mathcal{M}}(\boldsymbol{\rho}_n)$ denotes the set of grids above or on the path of the n-th data if $k_n = k^{(LOS)}$, otherwise, the set of grids below or on the path. And $\mu_n = \mu^{(LOS)}$ if $k_n = k^{(LOS)}$, otherwise, $\mu_n = \mu^{(NLOS)}$, where $\mu^{(LOS)}$ and $\mu^{(NLOS)}$ denote the updating rates for LOS and NLOS, respectively.

The hyperparameters $(\mu^{(LOS)}, \mu^{(NLOS)}, \lambda)$ are determined via cross-validation. Note that when $\mu^{(NLOS)} = 0.5$ and $\lambda \leq 0.5$, this process is the same as that in [10].

C. Prediction of the radio propagation environment

The propagation condition and the channel gain at a given RS-UE position pair $\boldsymbol{\rho}$ can be predicted using the estimated propagation parameters and the constructed blockage map. The propagation condition is predicted as follow.

$$\hat{k} = \begin{cases} k^{(LOS)}, & \max_{m \in \mathcal{M}(\boldsymbol{\rho})} p_m \leq 0.5 \\ k^{(NLOS)}, & otherwise \end{cases}, \quad (35)$$

where $\mathcal{M}(\boldsymbol{\rho})$ denotes the set of grids on the RS-UE path. The channel gain is calculated using the propagation parameters corresponding to the predicted propagation condition. The predicted channel gain is given by $\hat{\gamma} = -\alpha_{\hat{k}} D(\boldsymbol{\rho}) + \beta_{\hat{k}}$.

IV. Evaluation

A. Evaluation Assumptions

We conducted computer simulations to evaluate the prediction accuracy of the proposed method in an urban city area modeled in [14], where square buildings of width W are arranged in a two-dimensional array structure at equal intervals S in a square area of length L. We assumed that L = 200 [m], S = 20 [m], and W = 25 [m] based on the parameters in the urban scenario in [14]. The height of the buildings was given by the Rayleigh distribution with a mode of 15 [m] and restricted from 5 [m] to 35 [m].

The simulation assumptions are listed in Table I. The propagation parameters (α_k, β_k) were set according to the UMi street canyon model in [11], and a common shadowing deviation value $\bar{\sigma}$ was used for both LOS/NLOS. The RS measurement positions were uniformly distributed in the whole area, and the UEs were uniformly distributed in the area where there were no buildings. In the evaluation, assuming that a sufficient amount of data was collected over time, N_{RS} and N_{UE} were given as shown in the table. A study assuming a small number of data is a subject for future work.

TABLE I. SIMULATION ASSUMPTIONS

Parameter	Value
Antenna height	RS: 40 [m], UE: 1.5 [m]
Antenna configuration	8x8 URA (0.5 wavelength spacing)
Number of beams (B)	64
Propagation parameters	$\alpha_1 = 2.1, \beta_1 = -61.34$ $\alpha_2 = 3.53,\ \beta_2 = -53.22$ $\sigma_1 = \sigma_2 = \bar{\sigma}, \bar{\sigma} \in \{2,4,6\}$ [dB]
Channel parameters	$N_{path} = 12$, K-factor: 9 [dB] Azimuth angular spread: 15 [deg.] Zenith angular spread: 5 [deg.]
Number of training data	$N_{RS} = 49, N_{UE} = 4096$
Number of test data	$N_{RS} = 10, N_{UE} = 1000$

B. *Evaluation Results*

First, we evaluated the estimation accuracy of the propagation conditions. For comparison, a conventional method where the beam power ratio was not considered and $\pi_{n,k}$ was common for all data as in [7] was also evaluated. Fig. 3 shows the mean estimation error rate on the propagation conditions for the training dataset. Although the error rate of both methods is almost the same when $\bar{\sigma}$ is small, the error rate of the conventional method becomes much worse as $\bar{\sigma}$ increases. On the other hand, in the proposed method, the propagation conditions can be estimated accurately even when $\bar{\sigma}$ is large, since the beam power ratio is considered.

We then evaluated the root mean squared error (RMSE) between $\hat{\gamma}$ and $\bar{\gamma}$ as the prediction performance similar to [7]. In Fig. 4, the RMSE for the test dataset for both cases where λ was set to a value λ^* determined via cross-validation and where λ was fixed at 0.5 are plotted. Note that in the case where $\lambda = 0.5$, all data were used for the map construction without considering the responsibility. From Fig. 4, it can be seen that the proposed method can predict the channel gain with better accuracy than the conventional one. As $\bar{\sigma}$ increases, since the estimation accuracy becomes worse as shown in Fig. 3, the prediction accuracy also deteriorates greatly if the map is constructed using all data. However, by selecting data according to the responsibility, the prediction error is suppressed even in the case with a large $\bar{\sigma}$. When $\bar{\sigma} = 6$ dB, 'prop. ($\lambda = \lambda^*$)' can improve the RMSE of the channel gain by about 3.6 dB compared with 'conv. ($\lambda = 0.5$)'.

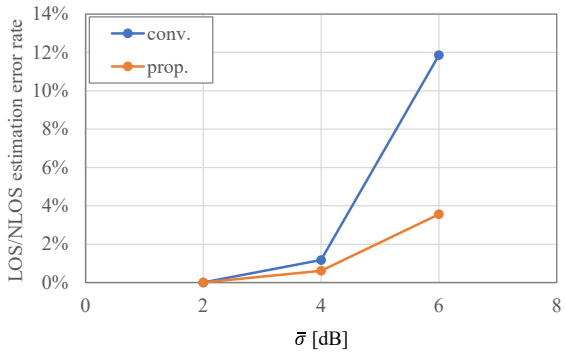

Fig. 3. The LOS/NLOS estimation error rate vs. $\bar{\sigma}$.

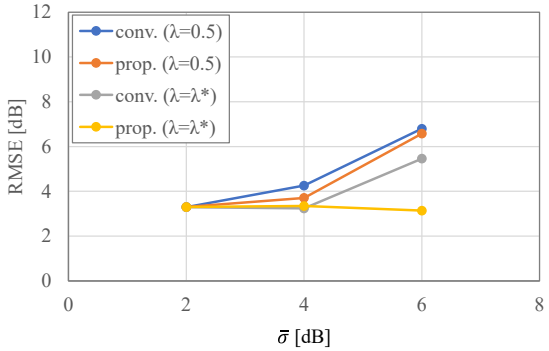

Fig. 4. The RMSE of the channel gain vs. $\bar{\sigma}$.

V. CONCLUSION

This paper proposed the radio propagation environment prediction method based on the received power information for multiple beams measured at various RS-UE position pairs in the UAV-assisted cellular network systems. The computer simulation results, assuming the urban environment, demonstrated that the proposed method can accurately predict the propagation environment even when there is a large variation in the received power.

ACKNOWLEDGMENT

This research is supported by the Ministry of Internal Affairs and Communications in Japan (JPJ000254).

REFERENCES

[1] A. Ghosh, A. Maeder, M. Baker and D. Chandramouli, "5G Evolution: A View on 5G Cellular Technology Beyond 3GPP Release 15," IEEE Access, Vol. 7, pp. 127639-127651, 2019.

[2] W. Jiang, B. Han, M. A. Habibi and H. D. Schotten, "The Road Towards 6G: A Comprehensive Survey," IEEE Open Journal of the Communications Society, Vol. 2, pp. 334-366, 2021.

[3] J. Park, S.-L. Kim and J. Zander, "Tractable Resource Management With Uplink Decoupled Millimeter-Wave Overlay in Ultra-Dense Cellular Networks," IEEE Transactions on Wireless Communications, Vol. 15, No. 6, pp. 4362-4379, 2016.

[4] S. Fujio and K. Ozaki, "UAV Deployment for MU-MIMO Capacity Maximization in UAV-assisted Cellular Networks with Millimeter-wave Beamforming," Proc. 2022 WPMC, 2022, pp. 244-249.

[5] P. Ladosz, H. Oh, G. Zheng and W.-H. Chen, "Gaussian Process Based Channel Prediction for Communication-Relay UAV in Urban Environments," IEEE Transactions on Aerospace and Electronic Systems, Vol. 56, No. 1, pp. 313-325, 2020.

[6] P. Zeng and J. Chen, "UAV-aided Joint Radio Map and 3D Environment Reconstruction using Deep Learning Approaches," Proc. 2022 IEEE ICC, 2022, pp. 5341-5346.

[7] J. Chen, U. Yatnalli and D. Gesbert, "Learning radio maps for UAV-aided wireless networks: A segmented regression approach," Proc. 2017 IEEE ICC, 2017, pp. 1-6.

[8] B. Zhang and J. Chen, "Constructing Radio Maps for UAV Communications via Dynamic Resolution Virtual Obstacle Maps," Proc. 2020 IEEE International Workshop on SPAWC, 2020, pp. 1-5.

[9] W. Liu and J. Chen, "Geography-aware Radio Map Reconstruction for UAV-aided Communications and Localization," Proc. 2021 IEEE ICC, 2021, pp. 1-6.

[10] O. Esrafilian, R. Gangula and D. Gesbert, "Map Reconstruction in UAV Networks via Fusion of Radio and Depth Measurements," Proc. 2021 IEEE ICC, 2021, pp. 1-6.

[11] 3GPP TR 38.901 V16.1.0, "Study on channel model for frequencies from 0.5 to 100 GHz," Dec. 2019.

[12] 3GPP TR 36.873 V12.7.0, "Study on 3D channel model for LTE," Dec. 2017.

[13] C. M. Bishop, Pattern recognition and machine learning, Springer, 2006.

[14] A. Al-Hourani, S. Kandeepan and A. Jamalipour, "Modeling air-to-ground path loss for low altitude platforms in urban environments," Proc. 2014 IEEE GLOBECOM, 2014, pp. 2898-2904.